SEPSIS

Amelioration of sepsis by TIE2 activation–induced vascular protection

Sangyeul Han,[1,2]*† Seung-Jun Lee,[2,3]† Kyung Eun Kim,[1]‡ Hyo Seon Lee,[1]‡ Nuri Oh,[3] Inwon Park,[4] Eun Ko,[1]‡ Seung Ja Oh,[1]§ Yoon-Sook Lee,[1]‡ David Kim,[3] Seungjoo Lee,[3] Dae Hyun Lee,[3] Kwang-Hoon Lee,[1]¶ Su Young Chae,[1]‡ Jung-Hoon Lee,[1]‡ Su-Jin Kim,[1]‡ Hyung-Chan Kim,[1]‡ Seokkyun Kim,[1]‡ Sung Hyun Kim,[1]|| Chungho Kim,[5] Yoshikazu Nakaoka,[6] Yulong He,[7] Hellmut G. Augustin,[8,9] Junhao Hu,[8] Paul H. Song,[1]‡ Yong-In Kim,[1]** Pilhan Kim,[4] Injune Kim,[3] Gou Young Koh[2,3]*

Protection of endothelial integrity has been recognized as a frontline approach to alleviating sepsis progression, yet no effective agent for preserving endothelial integrity is available. Using an unusual anti–angiopoietin 2 (ANG2) antibody, ABTAA (ANG2-binding and TIE2-activating antibody), we show that activation of the endothelial receptor TIE2 protects the vasculature from septic damage and provides survival benefit in three sepsis mouse models. Upon binding to ANG2, ABTAA triggers clustering of ANG2, assembling an ABTAA/ANG2 complex that can subsequently bind and activate TIE2. Compared with a conventional ANG2-blocking antibody, ABTAA was highly effective in augmenting survival from sepsis by strengthening the endothelial glycocalyx, reducing cytokine storms, vascular leakage, and rarefaction, and mitigating organ damage. Together, our data advance the role of TIE2 activation in ameliorating sepsis progression and open a potential therapeutic avenue for sepsis to address the lack of sepsis-specific treatment.

INTRODUCTION

Sepsis features overwhelming vascular inflammation and disintegration, particularly in lungs and kidneys, caused mainly by excessive pathogen (bacteria and virus) invasion into the circulation. It affects ~19 million people per year worldwide, with a high mortality (1, 2). Despite accumulating information about sepsis pathophysiology, general supportive care remains the pillar of treatment because aiming at a particular single therapeutic target for immunomodulatory or anticoagulant therapy has proven to be ineffective, probably because of the redundancy and heterogeneity of the host response to sepsis (3–5). To overcome such hurdles, vigorous vascular protection by controlling vascular inflammation before complete breakdown of endothelial integrity could be an effective therapy (3, 6–10). However, no satisfactory agent to induce vascular protection and concurrently inhibit inflammation has been developed.

The hallmarks of sepsis include a burst of diverse proinflammatory cytokine secretion, endothelial inflammation, systemic capillary leakage with tissue edema, and vasodilation refractory to vasopressors (1, 8, 9, 11, 12). Recent evidence has indicated that delaying sepsis progression by targeting the angiopoietin-TIE2 system for vascular and barrier stabilization is promising, but current options are ineffective and impractical (13–16). TIE2 agonists such as angiopoietin 1 (ANG1), the modified ANG1 variant "COMP-Ang1," and the TIE2-agonistic synthetic peptide "Vasculotide" have been reported to improve the devastating outcomes of sepsis (17–20). However, numerous hurdles remain related to production, purification, storage, half-life, and efficacy. For instance, we generated COMP-Ang1 (21) to overcome the drawbacks of native ANG1 protein as a possible therapeutic. COMP-Ang1 can be useful for promoting therapeutic angiogenesis in limited cases as a local therapy (22); however, it is quite difficult to use for therapeutic purposes such as treating sepsis through systemic administration in a controlled manner because of its very short half-life (23) and strong nonspecific binding to any tissue. Thus, a superior alternative TIE2 agonist has long been sought for systemic use. On the other hand, ANG2 mainly acts as a TIE2 antagonist in septic conditions and plays an augmenting role in vascular inflammation by promoting vascular leakage, leukocyte infiltration, and expression of vascular cell adhesion molecule–1 (VCAM-1), ultimately weakening the microvascular barrier (14, 16, 24–26). Circulating ANG2 is elevated in patients with sepsis, and this increased ANG2 concentration is closely correlated with severity and poor prognosis (27, 28). Accordingly, antibodies and small interfering RNAs (siRNAs) against Ang2 can delay septic progression in experimental sepsis models, but their efficacy is variable, presumably due to different approaches, modalities, and target organs for ANG2 inhibition (16, 29, 30).

Here, we present a TIE2-agonistic antibody, ABTAA, which robustly induces TIE2 activation and its downstream signaling by inducing ANG2 oligomerization. By applying ABTAA to several sepsis models for therapeutic purposes, we have unveiled the roles of simultaneous

[1]Samsung Advanced Institute of Technology, Suwon, 446-712, Republic of Korea. [2]Center for Vascular Research, Institute for Basic Science, Daejeon 305-701, Republic of Korea. [3]Graduate School of Medical Science and Engineering, Korea Advanced Institute of Science and Technology (KAIST), Daejeon 305-701, Republic of Korea. [4]Graduate School of Nanoscience and Technology, KAIST, Daejeon 305-701, Republic of Korea. [5]School of Life Sciences and Technologies, Korea University, Seoul 136-701, Republic of Korea. [6]Department of Cardiovascular Medicine, Osaka University Graduate School of Medicine, Suita, Osaka 565-0871, Japan. [7]Cyrus Tang Hematology Center, Soochow University, Suzhou 215123, China. [8]Division of Vascular Oncology and Metastasis, German Cancer Research Center Heidelberg (DKFZ-ZMBH Alliance), 69121 Heidelberg, Germany. [9]Department of Vascular Biology and Tumor Angiogenesis (CBTM), Medical Faculty Mannheim, Heidelberg University, 68167 Mannheim, Germany.
*Corresponding author. E-mail: gykoh@kaist.ac.kr (G.Y.K.); syhan69@gmail.com (S.H.)
†These authors contributed equally to this work.
‡Present address: Samsung Bioepis, Incheon 406-712, Republic of Korea.
§Present address: Samsung Biomedical Research Institute, Samsung Electronics Co. Ltd., Suwon 446-712, Republic of Korea.
¶Present address: New Drug Development Center, Osong Medical Innovation Foundation, Cheongju 363-951, Republic of Korea.
||Present address: Korea Institute of Ceramic Engineering and Technology, Seoul 153-801, Republic of Korea.
**Present address: Medytox, Pangyo Bioresearch Center, Seongnam-si 463-410, Republic of Korea.

ANG2 inhibition and TIE2 activation in vascular protection during sepsis progression and provided a rationale for clinical testing of ABTAA as an antibody for treating sepsis in patients.

RESULTS

ABTAA triggers TIE2 activation via ANG2/TIE2/ABTAA complex formation

In contrast to previously reported ANG2 antibodies that inhibit ANG2/TIE2 interaction (31–35), several ANG2 antibodies generated in our laboratories have displayed an unusual activity of triggering TIE2 phosphorylation without interrupting the ANG2/TIE2 interaction. One of these antibodies was selected and designated as ABTAA, a humanized monoclonal immunoglobulin G1 (IgG1) antibody (Fig. 1A). ABTAA could bind to human ANG2 with an equilibrium dissociation constant (K_D) value of 0.2 nM (fig. S1A) without inhibiting the ANG2/TIE2 interaction (fig. S1B). To further investigate and compare ABTAA's distinctive activity, we used a conventional ANG2-blocking antibody (ABA; K_D for human ANG2 = 78 pM) (fig. S1C), which inhibits the ANG2/TIE2 interaction [median inhibitory concentration (IC_{50}) = 0.22 nM] (Fig. 1A and fig. S1B). Both ABTAA and ABA cross-reacted with mouse ANG2 (K_D = 138 and 0.09 nM, respectively) (fig. S1D), but neither of these antibodies bound to ANG1 or inhibited ANG1/TIE2 interaction (fig. S1E).

In the presence of ANG2 in primary cultured human umbilical vein endothelial cells (HUVECs), ABTAA induced TIE2 phosphorylation in a dose-dependent manner, whereas ABA effectively inhibited ANG2-induced TIE2 phosphorylation like other conventional ANG2 antibodies (Fig. 1B). ABTAA + ANG2 also induced TIE2 translocation to cell-cell contact sites just like ANG1 (Fig. 1C). Furthermore, ABTAA + ANG2, but not ABA + ANG2, triggered the phosphorylation of diverse TIE2 downstream signals, including AKT and ERK (Fig. 1, D and E). ABTAA alone only negligibly triggered TIE2 downstream signaling (Fig. 1, D and E). TIE2 knockdown abolished AKT and ERK phosphorylation triggered by ABTAA + ANG2 (Fig. 1F). Consistent with a previous report showing FOXO1 localization in the cytoplasm after
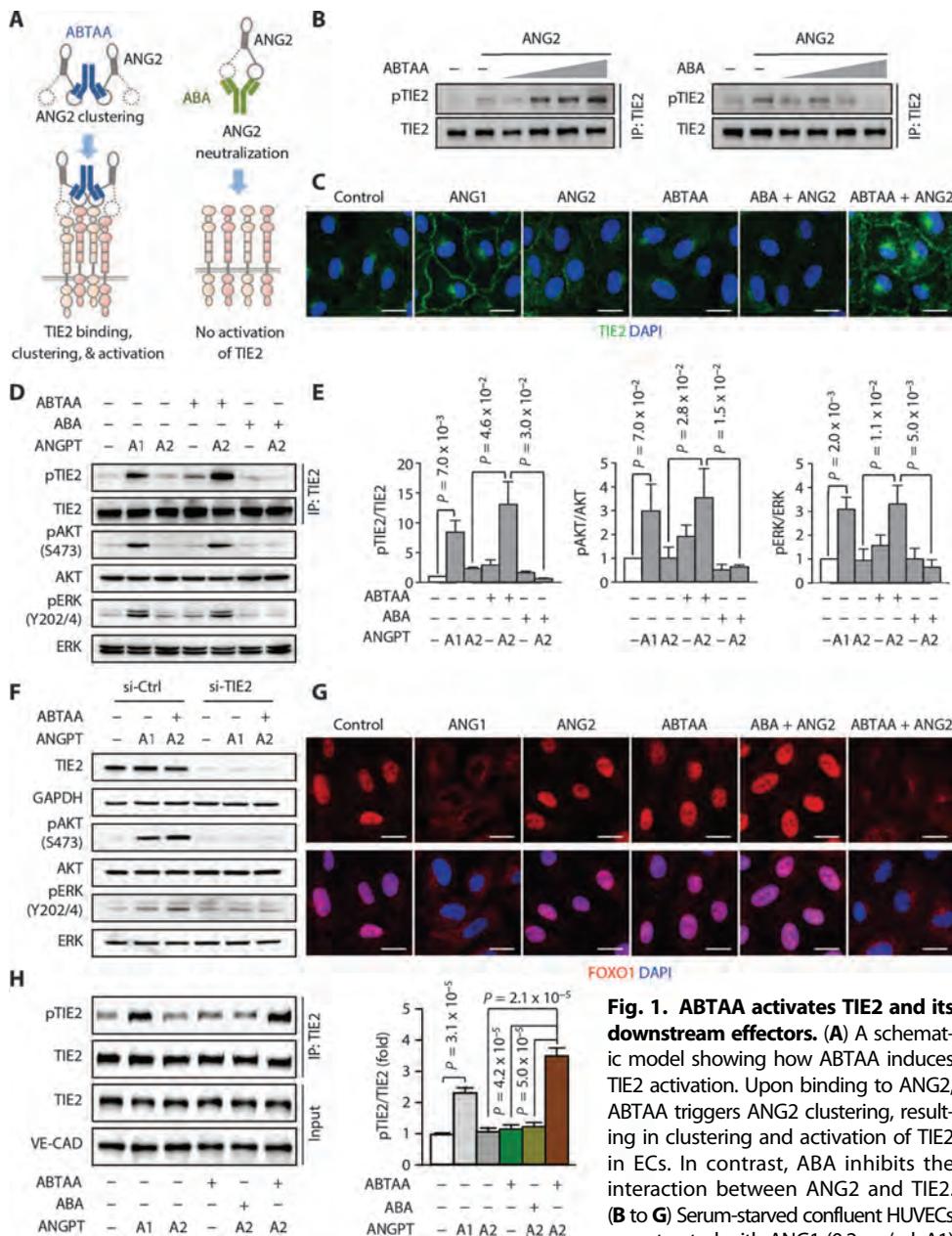
Fig. 1. ABTAA activates TIE2 and its downstream effectors. (**A**) A schematic model showing how ABTAA induces TIE2 activation. Upon binding to ANG2, ABTAA triggers ANG2 clustering, resulting in clustering and activation of TIE2 in ECs. In contrast, ABA inhibits the interaction between ANG2 and TIE2. (**B** to **G**) Serum-starved confluent HUVECs were treated with ANG1 (0.2 μg/ml; A1) or ANG2 (2 μg/ml; A2) along with ABTAA or ABA (10 μg/ml) for 30 min. (B) Amounts of TIE2 and phosphorylated TIE2 in serum-starved HUVECs that were treated with human ANG2 with or without ABTAA or ABA (0.01, 0.1, and 1, 10 μg/ml) for 15 min. HUVEC lysates were subjected to TIE2 immunoprecipitation (IP) and immunoblot analysis. (C) Confocal images showing that ABTAA induces TIE2 translocation to cell-cell contacts. Scale bars, 20 μm. DAPI, 4',6-diamidino-2-phenylindole. (D and E) Immunoblots and densitometric analysis for relative phosphorylation ratios of TIE2, AKT, and ERK (extracellular signal–regulated kinase) (means ± SEM, n = 3). ANGPT, angiopoietin. (F) Immunoblot detection of TIE2 and its downstream signaling in TIE2 siRNA-transfected HUVECs. (G) ABTAA-induced nuclear clearance of FOXO1. Scale bars, 50 μm. (**H**) In vivo TIE2 phosphorylation in the lung by ABTAA. Control phosphate-buffered saline, COMP-Ang1 (50 μg), ANG2 (20 μg), ABTAA (10 mg/kg) + ANG2 (20 μg), or ABA (10 mg/kg) + ANG2 (20 μg) were intravenously injected into wild-type mice. Lungs were sampled 2 hours after the treatment. Representative immunoblots showing phosphorylated TIE2 and total TIE2 in the IP samples and TIE2 and VE-cadherin (VE-CAD) in the lung lysates to validate the use of equal amounts for IP. Densitometric analysis (means ± SEM, n = 5) for relative phosphorylation ratios of TIE2 is shown. *P < 0.05 by one-way analysis of variance (ANOVA) followed by Student-Newman-Keuls post-test. Data are representative of three to five independent experiments.

phosphorylation (36), FOXO1, which was in the nucleus under the basal, serum-starved condition, became exclusively confined to the cytoplasm only with ABTAA + ANG2 or ANG1 (Fig. 1G). Similar findings were also observed in primary cultured human lung ECs (fig. S2), indicating that ABTAA can have an effect in multiple types of ECs. ABTAA induced TIE2 phosphorylation in vivo in lung ECs when administered to mice along with ANG2 (Fig. 1H). Together, these results indicate that ABTAA can regulate diverse endothelial signaling pathways via TIE2 activation.

We then investigated the mechanism by which ABTAA elicits TIE2 activation. Gel filtration analysis indicated that ANG2's fibrinogen-like domain (A2D; 276 to 496 amino acids, ~30 kD) and TIE2's extracellular domain (T2E; amino acids 1 to 452, ~55 kD) form a binary complex (Fig. 2A). When ABTAA (~160 kD) was mixed with the purified A2D/T2E complex, larger species appeared, composed of ABTAA, A2D, and T2E, as shown by SDS–polyacrylamide gel electrophoresis (SDS-PAGE). Multiangle light scattering (MALS) analysis of this complex revealed the existence of a homogeneous complex (302.7 kD) and suggested a 1:2 ratio between ABTAA and the A2D-T2E binary complex. Moreover, ABTAA specifically formed a complex with TIE2 only in the presence of ANG2 (Fig. 2B). ABTAA could be coimmunoprecipitated with both ANG2 and TIE2 in HUVECs (Fig. 2C), indicating that it can form a stable tripartite complex with TIE2 via ANG2 binding. Given that angiopoietin's oligomerization status is critical for TIE2 activation (14, 37, 38), we hypothesized that ABTAA can cause higher orders of ANG2 oligomerization by capturing multimeric ANG2. To test this idea, we generated a dimeric form of A2D (A2D-Fc; ~117 kD). When ABTAA was mixed with various amounts of A2D-Fc, a main peak with a molecular size of ~600 kD was commonly generated (Fig. 2D), which was far larger than the expected simple complex consisting of two A2D-Fc and one ABTAA (~390 kD). MALS analysis revealed that this purified complex existed predominantly with a molecular mass of ~677 kD along with several minor populations (998, 1330, or 1959 kD), supporting our notion that the distinct molecular function of ABTAA is attributable to the formation of a highly oligomerized ABTAA/ANG2 complex. Conversely, the Fab fragment of ABTAA, with only one ANG2 binding site, failed to induce TIE2, AKT, and ERK phosphorylation (Fig. 2, E to I). Additionally, immunofluorescence staining analysis showed that ABTAA induced TIE2 internalization and endocytosis (fig. S3A), and that the ABTAA/ANG2/TIE2 complex was traf-

ficked into endosomes (fig. S3, B and C), which is similar to the previously reported action of ANG1 (39) and ABA (35). On the basis of these data, we propose that ABTAA can form a multicomplex with ANG2, resulting in clustering, activation, and internalization of TIE2.
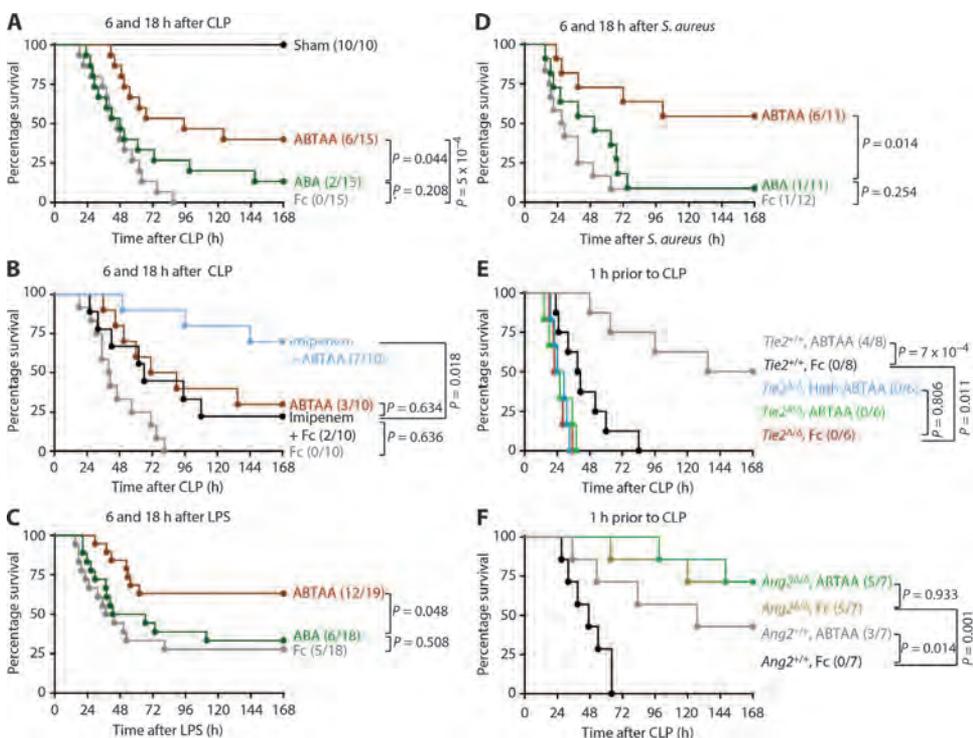
ABTAA reduces sepsis mortality

To examine whether ABTAA is better than ABA in improving survival in sepsis, we generated a severe sepsis model with a high-grade cecal ligation and puncture (CLP) (40) in adult C57BL/6 J mice. In an attempt to mimic a clinically relevant situation, we treated the mice with administrations of Fc, ABA, or ABTAA (10 mg/kg) at 6 and 18 hours after CLP (designated as "posttreatment"), and their survivals were monitored in a blind manner for 1 week. Compared with Fc (most of the mice treated with Fc died within 96 hours), ABTAA increased
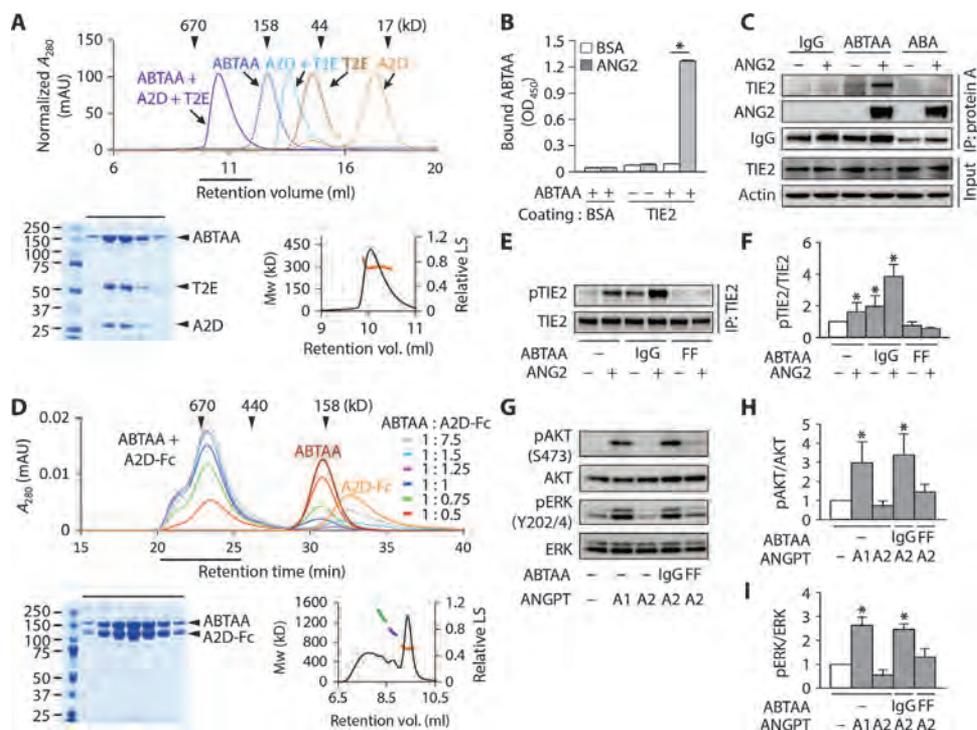
Fig. 2. ABTAA forms a stable complex with ANG2 and TIE2. (**A**) Size exclusion analysis of ABTAA, T2E, A2D, and the mixture of A2D and T2E with or without ABTAA. Relevant fractions were resolved in a nonreducing 4 to 12% SDS-PAGE gel (bottom left). MALS measurement of ABTAA bound to A2D-T2E showed the relative light scattering signal as a function of elution volume (bottom right). The measured molecular mass of ABTAA-A2D-T2E ternary complex is shown in orange (302.7 kD). A_{280}, absorbance of light at 280 nm; mAU, milli-absorbance unit. (**B**) Analysis of ANG2-dependent complex formation by enzyme-linked immunosorbent assay. Data are means ± SEM (n = 3). *P < 0.05 by Mann-Whitney U test. BSA, bovine serum albumin; OD_{450}, optical density at 450 nm. (**C**) Coimmunoprecipitation of ABTAA, ANG2, and TIE2 in HUVECs. Cell lysates were incubated with protein A beads to immunoprecipitate control IgG and antibodies. (**D**) Size exclusion analysis of ABTAA, A2D-Fc, and the mixtures of these two proteins with the indicated molar ratios. SDS-PAGE (bottom left) and MALS (bottom right) analyses of ABTAA–A2D-Fc complex showed the existence of higher oligomeric states (orange, 677 kD ± 0.28%; purple, 998 kD ± 0.14%; green, 1330 kD ± 0.12%). The measured molecular mass of the highest multimer (1959 kD) is omitted for clarity. (A and D) Arrowheads indicate the elution positions of the following size marker proteins: thyroglobulin (670 kD), ferritin (440 kD), aldolase (158 kD), ovalbumin (44 kD), and myoglobulin (17 kD). (**E** to **I**) HUVECs were treated with ANG1 (0.2 µg/ml; A1) or ANG2 (2 µg/ml; A2) along with ABTAA or its Fab fragment (FF) (10 µg/ml) for 30 min. Immunoblot and densitometric analyses showed that Fab fragment of ABTAA fails to phosphorylate TIE2 and its downstream effectors, AKT and ERK, in cultured HUVECs. Bars indicate means ± SEM (n = 3). *P < 0.05 by one-way ANOVA followed by Student-Newman-Keuls post-test.

the survival rate to ~40% at 1 week, whereas ABA improved it only to ~13% (Fig. 3A).

No further improvement in survival was detected with a higher dose (25 mg/kg) of ABA (fig. S4A). Because ABTAA has no direct effect on bacterial dissemination, we added the broad-spectrum antibiotics imipenem/cilastatin (20 mg/kg) to the ABTAA treatment 6 hours after CLP. Encouragingly, the combination of ABTAA and antibiotics enhanced survival to ~70%, whereas antibiotics improved it only to ~20% (Fig. 3B). The survival benefit of ABTAA was also superior in a preventive setting (single administration of antibody 1 hour before CLP, designated as "pretreatment"), which improved the survival rate to 50% compared with ABA (17%; fig. S4B). We also investigated the survival benefit of double administrations of ABTAA (10 mg/kg; each at 6 and 18 hours after the challenge) in two other sepsis models: endotoxemia [LD_{75} (75% lethal dose) of gram-negative endotoxin lipopolysaccharide (LPS)] and bacteremia (LD_{90} of *Staphylococcus aureus*). In the endotoxemia model, ABTAA increased the survival rate to 63%, whereas ABA and Fc survival rates were 33 and 28%, respectively (Fig. 3C). Similarly, ABTAA increased the survival rate to 55% compared with 9 and 8% survival rates for ABA and Fc, respectively, in the bacteremia model, indicating that ABTAA could be an antiseptic therapeutic antibody that is effective for various causes of sepsis (Fig. 3D).

Long-term TIE2 activation is crucial in the ABTAA-induced ameliorating effect in sepsis

To delineate the involvement of angiopoietin-TIE2 signaling in ABTAA's effect, we tested it further using *Ang1*-, *Ang2*-, or *Tie2*-depleted mouse models. First, *Ang1*-depleted mice ($Ang1^{\Delta/\Delta}$) were quite susceptible to CLP, exhibiting higher mortality rates with a median survival of 18.5 hours compared with control mice (43.2 hours) (fig. S4C). Pretreatment with ABTAA (10 mg/kg) resulted in a negligible survival benefit in $Ang1^{\Delta/\Delta}$, but it increased long-term survival (50%) in control mice. However, median survival of the $Ang1^{\Delta/\Delta}$ mice significantly increased ($P = 3.0 \times 10^{-4}$) from 18.5 to 55.0 hours when ABTAA dose was increased to 25 mg/kg (fig. S4C), implying that basal TIE2 signaling might be attenuated in $Ang1^{\Delta/\Delta}$ animals, and that the dosage of ABTAA needs to be elevated to maintain TIE2 expression and activation in septic conditions. $Ang1^{\Delta/\Delta}$ mice exhibited markedly reduced TIE2 phosphorylation (Y992) in lung ECs compared with $Ang1^{+/+}$ control mice (fig. S5, A and B). Notably, ABTAA increased the amount of phosphorylated TIE2 in $Ang1^{+/+}$, but it exerted negligible effects in $Ang1^{\Delta/\Delta}$ mice (fig. S5, A and B). However, a higher dosage of ABTAA (25 mg/kg) evoked modest TIE2 phosphorylation (fig. S5, A and B), which could be the explanation for the improved survival observed in $Ang1^{\Delta/\Delta}$.

Tie2-depleted mice ($Tie2^{\Delta/\Delta}$), compared with control mice, were more susceptible to CLP, showing higher mortality with a median survival of 23.5 hours (Fig. 3E), which is consistent with a previous report that used heterozygous *Tie2*-deficient mice (41). ABTAA treatment (10 mg/kg) in $Tie2^{\Delta/\Delta}$ did not provide any survival benefit, and even a higher dosage of ABTAA could not rescue the high mortality rates of $Tie2^{\Delta/\Delta}$ animals. These findings all indicate that TIE2 activation has an integral function in ABTAA-induced rescue of severe sepsis mortality.

We also used *Ang2*-depleted mice ($Ang2^{\Delta/\Delta}$) (fig. S6) to confirm that ABTAA relies on ANG2 for TIE2 activation. As predicted, ABTAA provided no additional survival benefit in $Ang2^{\Delta/\Delta}$ compared with Fc-treated mice (Fig. 3F), indicating that ANG2 is essential for ABTAA's action. Additionally, ANG2 seems to be a critical factor in sepsis progression, considering that $Ang2^{\Delta/\Delta}$ animals showed notably higher survival than wild-type mice, consistent with a previous report on $Ang2^{+/-}$ (26).

To address whether long-term TIE2 activation is required for effective amelioration of sepsis, we compared the survival rate in the groups pretreated with another TIE2 agonist, COMP-Ang1 (a short half-life) (23), or ABTAA (a long half-life) in two sepsis models. Our side-by-side comparison revealed that the β phase half-life ($t_{1/2}$, β) of COMP-Ang1 in the blood was ~30 min, whereas that of ABTAA was ~198 hours (fig. S7A). Although ABTAA again improved survival (~45 to 60%),

Fig. 3. ABTAA rescues mice from sepsis in ANG2/TIE2-dependent manner. (**A** to **D**) Survival curves of wild-type mice with intravenous administration of Fc, ABA, or ABTAA (10 mg/kg each) at 6 and 18 hours after CLP, intraperitoneal LPS injection, or intraperitoneal *S. aureus* inoculation. (B) Survival curves of wild-type mice treated with ABTAA and/or broad-spectrum antibiotics. For the combined treatment settings, imipenem/cilastatin (20 mg/kg) was administered six times every 12 hours starting at 6 hours after CLP to the mice treated with Fc or ABTAA (10 mg/kg) at 6 and 18 hours after CLP. (**E** and **F**) Fc or ABTAA (10 mg/kg) was administered to $Tie2^{\Delta/\Delta}$ or $Ang2^{\Delta/\Delta}$ mice and their littermate controls 1 hour before CLP. High dosage (25 mg/kg, high) of ABTAA was also administered to $Tie2^{\Delta/\Delta}$ mice. Numbers in parentheses represent the number of surviving mice out of total mice tested for each group. Statistical significance was analyzed by a log-rank test.

two administrations of COMP-Ang1 (10 mg/kg) provided a poor improvement in survival in CLP (~17%) and endotoxemia (~3%) (fig. S7, B and C). Thus, long-term TIE2 activation is crucial for the ABTAA-induced ameliorating effect in severe sepsis.

ABTAA preserves the parenchyma and vasculature integrity of major vital organs

To characterize how ABTAA improves overall survival, we analyzed the changes in the blood vessels of major organs in the posttreatment setting during sepsis. Because the lung is a major target organ of sepsis, we carried out a vital micro-CT (computed tomography) analysis to trace the therapeutic effect of ABTAA in reducing pulmonary edema, which can be indirectly measured by the leakage area in the whole lung during endotoxemia-induced septic progression (Fig. 4, A and B). Compared with Fc, ABTAA markedly suppressed lung edema by 60% at 30 hours after endotoxin injection, whereas ABA had no effects in alleviating edema (Fig. 4, B and C). Moreover, at 24 hours after CLP, ABTAA attenuated typical sepsis-induced acute lung injury, which consists of inter-alveolar thickening, filling with exudate, and intra-alveolar cell infiltration, compared with ABA (Fig. 4D). Semi-quantitative pulmonary histological scoring further revealed that ABTAA-treated mice had significantly preserved parenchymal integrity compared with ABA-treated ($P = 3.8 \times 10^{-3}$) or Fc-treated ($P = 3.0 \times 10^{-3}$) mice (Fig. 4E). In septic mice treated with Fc, pulmonary microvessels showed a loss of NG2+ pericyte coverage by 75% (Fig. 4, D and F), which presumably was caused by severe impairment of the EC-pericyte interaction resulting from severe inflammation and EC damage. However, ABTAA alleviated pericyte loss by 45%, whereas ABA had no significant effect (Fig. 4, D and F). Thus, TIE2 activation attenuates pericyte loss by reversing the EC-pericyte disintegration. Renal cortex also exhibited mitigation of parenchymal damage by ABTAA but not by ABA (fig. S8, A and B). In addition, renal peritubular capillary rarefaction was observed in the Fc-treated mice, which had ~50% of the microvascular density relative to the sham controls; this was ameliorated by ABTAA to 66% (fig. S8, A and C). Furthermore, Fc-treated septic mice showed loss and disorganization of VE-cadherin (49% standardized to sham) in the thoracic aorta, which was recovered by ABTAA (65%) but not by ABA (fig. S8, A and D). Pretreatment with ABTAA also markedly reduced organ injuries and protected microvascular integrity in mice with CLP-induced sepsis, whereas ABA induced improvements but to a lesser extent (fig.

S9, A to F). In addition, mice treated with ABTAA generally looked healthy, whereas mice treated with Fc or ABA looked severely lethargic at 24 hours after CLP (movie S1). These results indicate that TIE2 activation–induced preservation of microvascular integrity mitigates parenchymal deterioration of major vital organs during the early phase of septic progression, and that simply blocking ANG2 is insufficient to preserve microvascular integrity.

ABTAA protects endothelial glycocalyx during sepsis
Endothelial glycocalyx, mainly composed of heparan sulfate (HS) and proteoglycan, serves as a crucial barrier that prevents the adhesion of blood cells onto the endothelial surface (42) and that is lost during sepsis because of heparanase and tumor necrosis factor–α (TNF-α) effects (43). In contrast, ANG1 increases the depth of endothelial glycocalyx by increasing glycosaminoglycan content (44). Therefore,
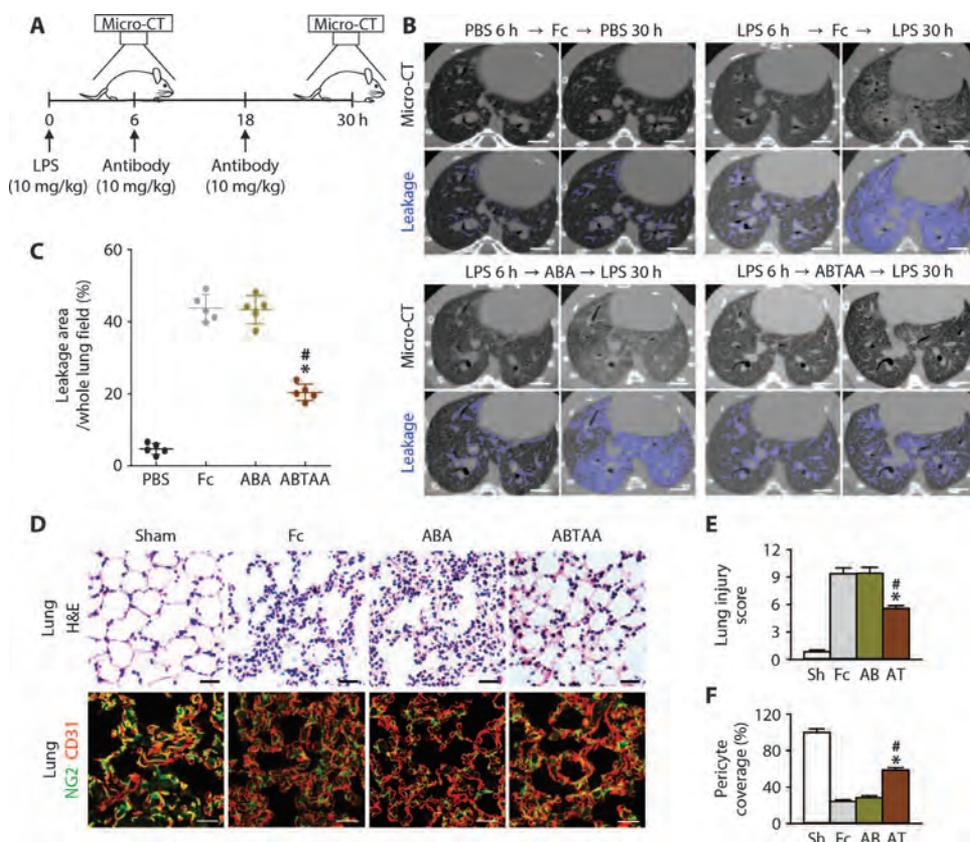

Fig. 4. ABTAA prevents the progression of acute lung injury by reducing vascular leakage, inflammation, and pericyte detachment. (**A** to **C**) Wild-type mice were inoculated with LPS (10 mg/kg, intraperitoneally) and underwent a micro-CT scan at 6 hours after LPS for the confirmation of mild pulmonary edema. Immediately and 12 hours after the micro-CT scanning, mice were treated with Fc, ABA, or ABTAA (10 mg/kg) and underwent a follow-up micro-CT scan at 30 hours after LPS inoculation. (A) Experimental scheme for vital tracing of pulmonary edema using micro-CT and treatments. (B and C) Representative images and comparisons of pulmonary vascular leakage at 6 and 30 hours after LPS. Micro-CT images were pseudocolored with blue for measurements of leakage areas. Scale bars, 2 mm. Bars indicates mean ± SEM (each group, n = 5). (**D** to **F**) Fc, ABA (AB), or ABTAA (AT) (10 mg/kg) was given to mice at 6 and 18 hours after CLP, and the lungs were harvested 24 hours after CLP. Representative images and comparisons are shown for lung parenchymal injuries and pericyte coverage (which is presented as the relative percentage of NG2+ area per CD31+ area). Scale bars, 20 μm. Bars indicate means ± SEM (each group, n = 4 to 5). *P < 0.05 versus Fc; #P < 0.05 versus AB. Sh, sham. The P values were determined by one-way ANOVA followed by Student-Newman-Keuls post-test. H&E, hematoxylin and eosin.

we investigated whether posttreatment with ABTAA could preserve endothelial glycocalyx. We estimated the depth of endothelial glycocalyx by measuring a red blood cell exclusion zone in the subpleural microvasculature with intravital microscopy (fig. S10A). At 24 hours after CLP, this depth was markedly reduced compared with sham-operated mice (1.61 ± 0.26 μm versus 0.83 ± 0.12 μm; fig. S10, B and C). However, ABTAA clearly preserved the depth (~1.2 μm), whereas ABA showed a negligible effect (Fig. 5, A and B). We next examined the expression of HS in the lung microvasculature and perlecan in renal glomeruli (Fig. 5C). At 24 hours after CLP, the relative densities of HS and perlecan were significantly reduced by 72% ($P = 5.9 \times 10^{-3}$) and 70% ($P = 1.8 \times 10^{-3}$), respectively. However, ABTAA treatment protected against the degradation of HS and perlecan by 43 and 48%, respectively, whereas ABA showed no significant effect (Fig. 5, D and E). In line with

these results, the expression of heparanase was increased by 6.0- and 9.5-fold in the lungs and glomeruli of Fc-treated mice at 12 hours after CLP, respectively, compared with sham-operated mice (Fig. 5, F to H); however, ABTAA suppressed the up-regulation of heparanase in the lungs and glomeruli by 83 and 64%, respectively. Heparanase expression was robustly increased in the lung vasculature of both $Ang1^{\Delta/\Delta}$ and $TIE2^{\Delta/\Delta}$ animals, and the elevated heparanase in $TIE2^{\Delta/\Delta}$ was unaffected by ABTAA (Fig. 5, I and J), indicating that TIE2 activation is crucial for suppressing sepsis-induced up-regulation of heparanase.

ABTAA lessens neutrophil infiltration and improves vascular function during sepsis

Given that devastating and uncontrolled vascular leakage is one of the main factors in sepsis-induced mortality (6), we also aimed to evaluate
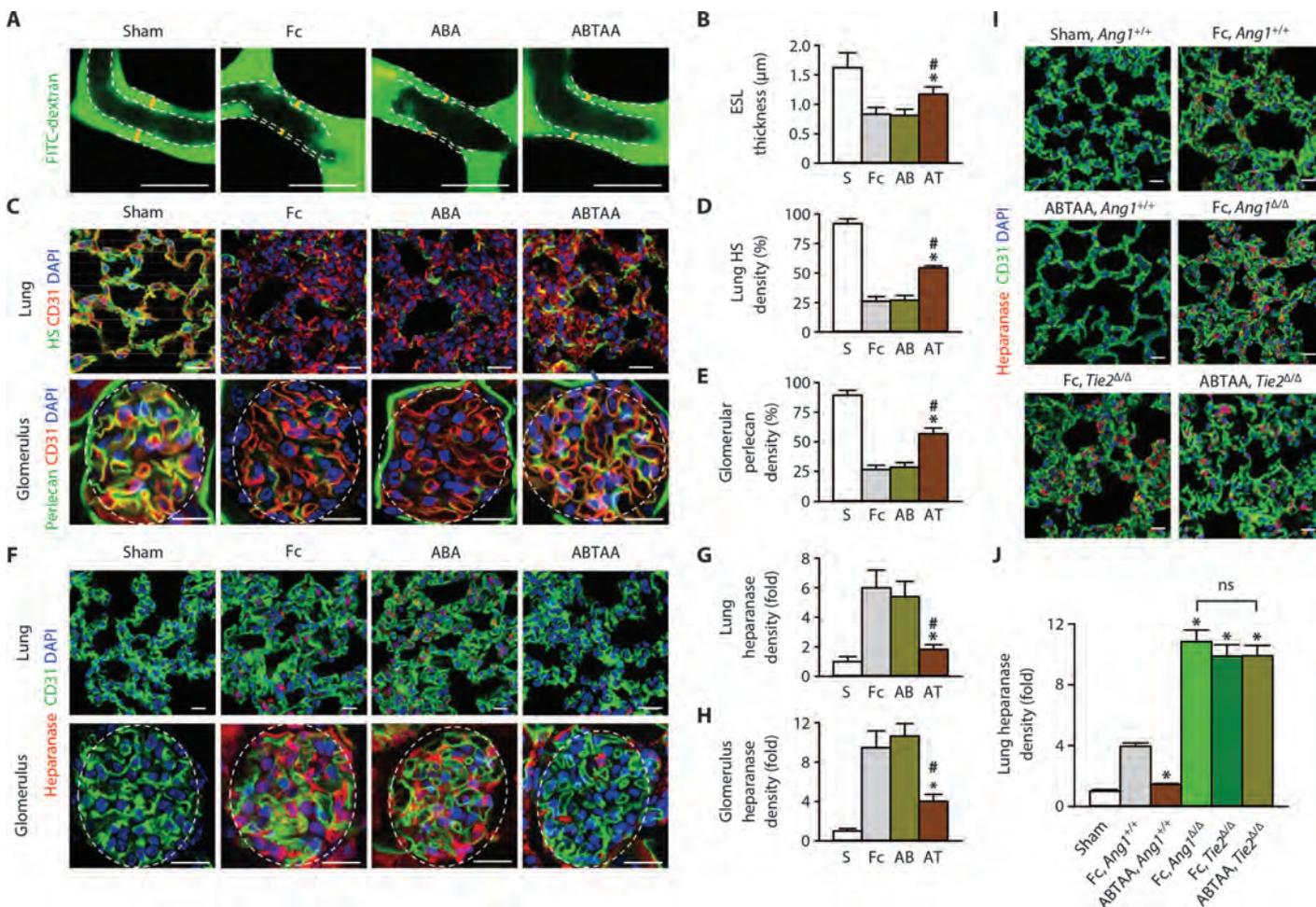
Fig. 5. ABTAA-induced TIE2 activation preserves endothelial glycocalyx. (**A** to **H**) Fc, ABA (AB), or ABTAA (AT) (10 mg/kg) was given to mice at 6 hours after CLP. (A) Representative images of intravital microscopy showing the thickness (yellow solid bar) of endothelial surface layer (ESL) measured by subtracting the width of the red blood cell track (inner dotted line) from the capillary diameter (outer dotted line) of subpleural pulmonary microvasculature. Fluorescein isothiocyanate (FITC)–dextran was intravenously injected at 24 hours after CLP, and the fluorescence images were acquired through a lung window. Scale bars, 10 μm. (B) Quantitative analysis of ESL thickness. Ten random images from four mice per group were analyzed in a blind manner. S, sham. (C to E) Representative images and

comparisons of relative densities of HS and perlecan in lungs and renal glomeruli that were harvested 24 hours after CLP. (F to H) Representative images and comparisons of relative densities of heparanase in lungs and renal glomeruli that were harvested 12 hours after CLP. (I and J) Wild-type, $Ang1^{\Delta/\Delta}$, or $Tie2^{\Delta/\Delta}$ mice were treated with Fc or ABTAA (10 mg/kg) 1 hour before CLP, and the lungs were harvested 12 hours after CLP. Representative images and comparisons of heparanase densities are presented. Dotted circle, glomerulus. *$P < 0.05$ versus Fc or Fc, $Ang1^{+/+}$; #$P < 0.05$ versus AB. Scale bars, 20 μm. ns, not significant. Bars indicate means ± SEM (each group, $n = 3$ to 4). The P values were determined by one-way ANOVA followed by Student-Newman-Keuls post-test.

the effects of ABTAA on vascular permeability. In confluent HUVECs, addition of TNF-α (1 ng/ml) resulted in gap formation caused by disrupted cell-cell contact, indicative of breakdown of the endothelial barrier. The formation of intercellular gaps or focal adhesions was deterred by ABTAA + ANG2 or ANG1 (Fig. 6A). Furthermore, ABTAA + ANG2 suppressed the TNF-α–induced passage of FITC-dextran through endothelial gaps in the in vitro permeability assay (Fig. 6B). Also, as shown in Fig. 6C, both ABTAA + ANG2 and ANG1 inhibited TNF-α–induced myosin light chain (MLC) phosphorylation, whereas vehicle control and ANG2 alone did not. These results indicate that ABTAA + ANG2–induced TIE2 activation can inhibit endothelial contraction through inhibiting the phosphorylation of MLC, thus stabilizing endothelial integrity, which replicates the effect of ANG1. Both Evans blue dye and FITC-conjugated dextran leakage analyses revealed that ABTAA counteracted vascular leakage more effectively than ABA in the lungs of the CLP model (Fig. 6D and fig. S11, A and B). In primary cultured HUVECs, ABTAA + ANG2, like ANG1, effectively suppressed the mRNA expression of the proinflammatory adhesion molecules ICAM-1, VCAM-1, and E-selectin in response to TNF-α stimulation in HUVECs (Fig. 6E). Accordingly, ABTAA, but not ABA, profoundly reduced Gr-1⁺ neutrophil infiltration into the lungs during sepsis (Fig. 6, F and G).

From these results, we inferred that the preservation of endothelial glycocalyx and the suppression of adhesion molecules by ABTAA complementarily attenuate sepsis-induced neutrophil adhesion to lung microvasculature. Moreover, ABTAA strikingly improved the perfusion of FITC-lectin into the lung microvasculature and renal glomeruli in septic mice by 57 and 47%, whereas ABA had negligible effects (Fig. 6, H and I). Thus, these results support our hypothesis that ABTAA-induced TIE2 activation can be a powerful mediator for lessening sepsis-induced abnormal vascular permeability and neutrophil infiltration in the lungs and EC damage.

ABTAA blunts cytokine storm and surge of circulating ANG2

In the early phase of sepsis, an excessive and uncontrolled release of proinflammatory cytokines (cytokine storm) causes pathologic alterations of leukocytes and ECs and deregulated vascular permeability (45). Consistently, serum TNF-α and IL-6 (interleukin-6), which are representative cytokines, were elevated by 6 hours after CLP (Fig. 7, A and B). Pre- and posttreatment
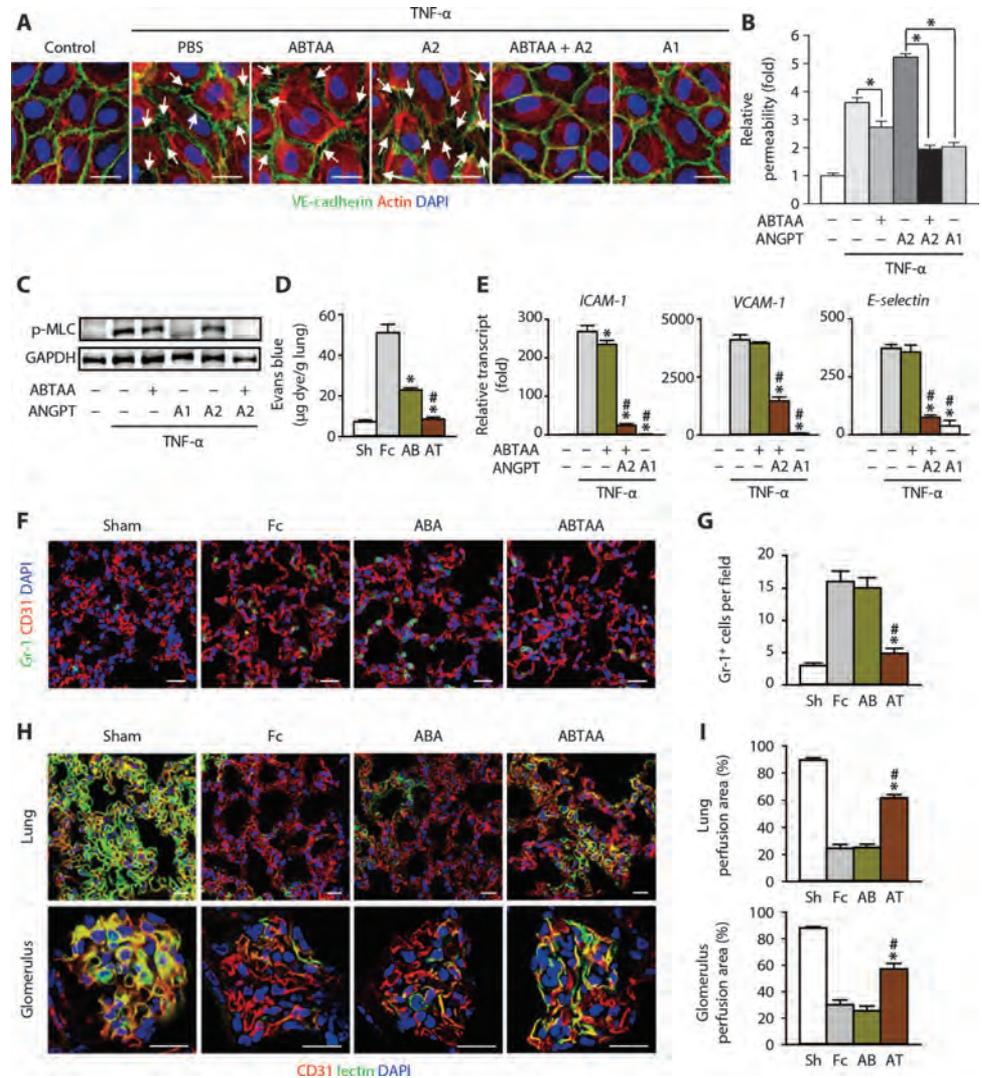

Fig. 6. ABTAA suppresses sepsis-induced hyperpermeability and neutrophil adhesion and improves vascular perfusion. (A to C and E) Confluent HUVECs, pretreated with ANG1 (A1) or ANG2 (A2) with or without ABTAA for 30 min, were analyzed 6 hours after stimulation with TNF-α. (A) Representative images of HUVECs stained with VE-cadherin or actin. Arrows indicate inter-endothelial gaps. Scale bars, 20 μm. (B) Permeability was quantified in TNF-α–stimulated HUVECs by determining the relative ratios of FITC-dextran leakage (each group, n = 3). *P < 0.01 versus ANG2 + TNF-α. (C) Immunoblot analysis shows a decrease in phospho-MLC (Thr¹⁸/Ser¹⁹) after A1 or ABTAA + A2 treatment in TNF-α–treated HUVECs. (D) In vivo Evans blue permeability assay shows the superior efficacy of ABTAA in reducing vascular leakage in lungs compared with ABA (each group, n = 6, pretreatment setting). Each antibody (10 mg/kg) was given 1 hour before CLP. (E) Quantitative reverse transcription polymerase chain reaction analysis shows that ABTAA suppressed the up-regulation of inflammatory adhesion molecules in TNF-α–treated HUVECs. Expression of ICAM-1, VCAM-1, and E-selectin mRNAs was normalized to HPRT-1 (each group, n = 4). *P < 0.05 versus TNF-α; #P < 0.05 versus TNF-α + ABTAA. (F to I) Fc, ABA (AB), or ABTAA (AT) (10 mg/kg) was given at 6 hours after CLP, and lungs, kidneys, and blood samples were collected 24 hours after CLP. (F and G) Representative images and comparison of neutrophil infiltration into the lungs quantified by immunofluorescence density of the granulocyte marker Gr-1 (each group, n = 7). (H and I) Representative images and comparisons of FITC-lectin perfusion in lungs and renal glomeruli (each group, n = 4 to 5). Scale bars, 20 μm. *P < 0.05 versus Fc; #P < 0.05 versus AB. All bars indicate means ± SEM. The P values were determined by one-way ANOVA followed by Student-Newman-Keuls post-test.

with ABTAA blunted their concentrations by 45 to 89% and 25 to 75%, respectively, but ABA had no effect in the CLP model (Fig. 7, A and B, and fig. S12, A and B). In contrast, although ABTAA improved survival (Fig. 3C), it did not significantly change cytokine concentrations in the endotoxemia model (fig. S13, A and B). These findings imply that ABTAA-induced dampening of the cytokine storm might result from reduced recruitment of inflammatory cells to the CLP region, and that this feature partly contributes to impeding further severe inflammation and mortality.

Because circulating ANG2 is one of the key biomarkers for sepsis severity and ANG2 itself contributes to sepsis progression (46, 47), we monitored circulating ANG2 concentrations in septic mice. Basal circulating ANG2 concentration was ~4.0 ng/ml, and it progressively increased until it peaked at 12 hours after CLP (~74 ng/ml) and gradually decreased afterwards (Fig. 7C and fig. S14). Posttreatment with ABTAA blunted the increment of circulating ANG2 after CLP by 32 to 48% (Fig. 7C). This trend was similarly observed even in the pretreatment setting (fig. S14). We attribute the ABTAA-induced reduction of circulating ANG2 to two processes: (i) enhanced ANG2 removal from circulation by rapid endocytosis and degradation in endothelium, (ii) and suppression of ANG2 secretion from the inflamed endothelium. ABTAA was highly detected in the cytoplasm of lung ECs, whereas Fc and ABA were barely detected (Fig. 7, D and E). Moreover, imipenem/cilastatin pretreatment alone similarly affected the circulating ANG2 concentrations (fig. S14), possibly because it suppresses bacteria-induced inflammation. In contrast, both post- and pretreatment with ABA increased circulating ANG2 concentrations (Fig. 7C and fig. S14), which could be attributable to ABA's ability to simply sequester ANG2 rather than promoting its clearance. We noted that although ~90% of circulating ANG2 was antibody-bound in mice posttreated with ABA, the actual concentration of free-form ANG2 was greater in ABA-treated mice than ABTAA-treated mice (Fig. 7F). Similar results were also detected in the mice posttreated with another type of ABA "REGN910 (34)" (Fig. 7F). Together, these data indicate that ABTAA has a robust ability to effectively clear ANG2 from circulation unlike ABA. Thus, ABTAA provides additional advantages in protecting vascular integrity by reducing both sepsis-induced cytokine storm and circulating ANG2.
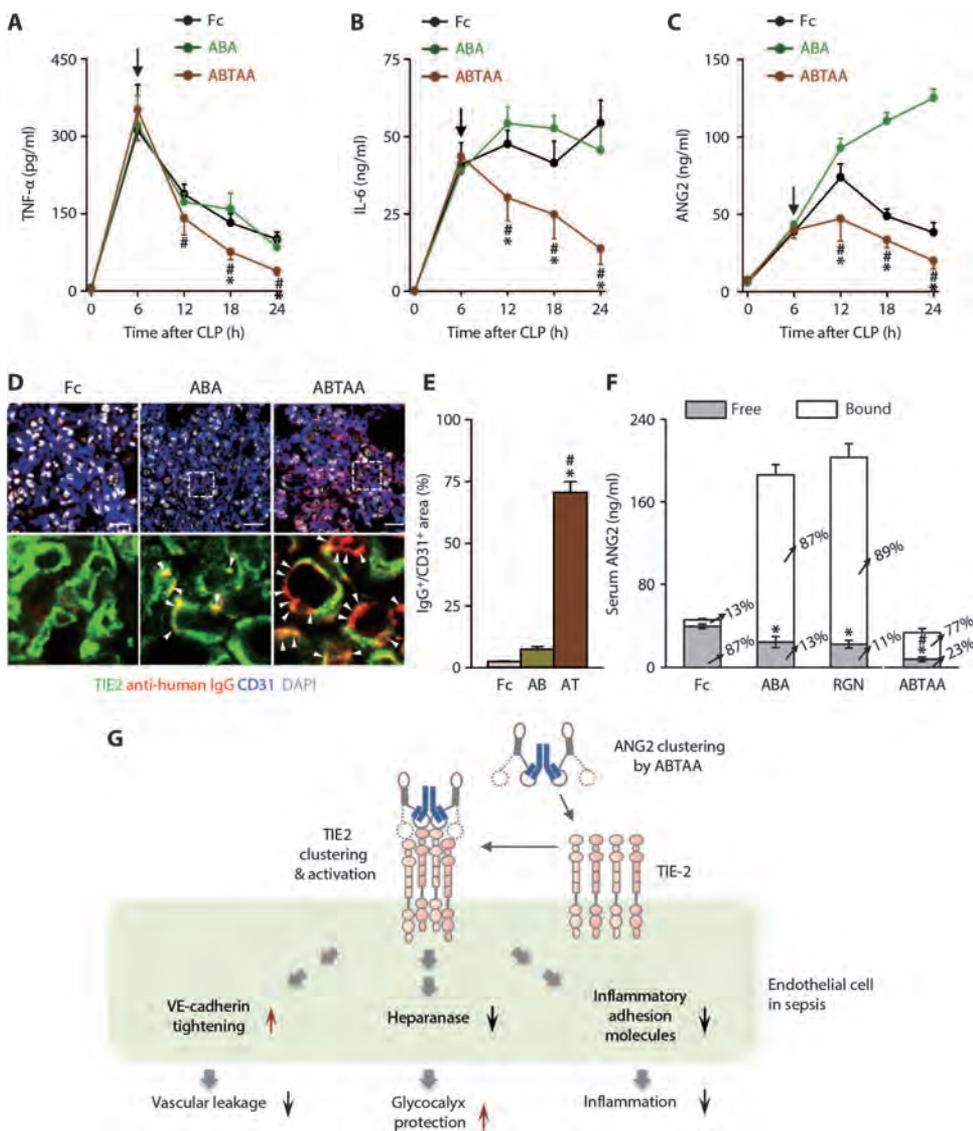
Fig. 7. ABTAA blunts cytokine storm and ANG2 surge in sepsis. (A to E) Fc, ABA (AB), or ABTAA (AT) (10 mg/kg) was given at 6 hours after CLP (indicated by arrows), and blood samples and lungs were collected at indicated time points. (A to C) Temporal changes of TNF-α, IL-6, and ANG2 concentrations in serum after CLP (each group, $n = 6$ to 8). (D and E) Representative images and comparison (each group, $n = 3$ to 4) of colocalization of Fc, ABA, or ABTAA with lung ECs (arrowheads). Lungs were harvested at 2 hours after antibody injection, and the injected antibodies were directly detected by anti-human IgG secondary antibody. (F) Total, free, and antibody-bound ANG2 in serum at 18 hours after CLP with pretreatment of Fc, ABA, REGN 910 (RGN), or ABTAA (10 mg/kg) 1 hour before CLP. Each group, $n = 5$ to 6. (G) A schematic model showing how ABTAA induces ANG2 clustering, resulting in clustering and activation of TIE2 receptors on ECs in sepsis. Ultimately, ANG2 sequestering and TIE2 activation by ABTAA reduces vascular leakage, protects glycocalyx, and suppresses inflammatory responses. Scale bars, 20 μm. Bars indicate means ± SEM. *$P < 0.05$ versus Fc; #$P < 0.05$ versus AB.

DISCUSSION

The present study demonstrates vascular protection by TIE2 activation as a promising therapeutic strategy in fighting sepsis. We used genetically modified mice and intravital imaging and found that TIE2

activation by ABTAA plays a pivotal role in ameliorating sepsis, mainly through preserving endothelial glycocalyx and microvascular integrity of major vital organs and inhibiting vascular leakage and cytokine storm (Fig. 7G).

Furthermore, when combined with antibiotics, ABTAA markedly enhanced survival from sepsis. It would be interesting to test the combined effect of ABTAA with other immune modulatory agents/devices, including the Toll-like receptor 4 (TLR4) antagonist eritoran (48), HMGB1 blocker (49), TNF-α inhibitor (50), anticoagulants such as activated protein C (51), or an extracorporeal blood-cleansing device (52).

Compared with the previously reported ABAs (31–35), ABTAA has a very distinctive property in that it can transform an antagonistic or very weakly agonistic ligand ANG2 into a strong agonist to its own receptor TIE2, thus activating TIE2 robustly by forming the tripartite ABTAA/ANG2/TIE2. ABTAA has a distinctive mode of action of clustering ANG2 without interfering with ANG2's interaction with its receptor TIE2, which greatly differs from the current prevailing rationale of developing a therapeutic antibody that prevents ligand-receptor binding. With this mechanism, ABTAA also efficiently exhausts circulating ANG2 through "capture and endocytosis" into ECs by binding and activating TIE2. This mode of action provides a way of scavenging harmful, excess ANG2 in the septic condition. Elucidation of the complex structure and epitope mapping will be necessary to reveal the detailed molecular mechanism underlying how ABTAA binds to ANG2 without interrupting the ANG2/TIE2 interaction. We propose that ABTAA binds to a certain portion within A2D (269 to 496 amino acid residues), which is separate from the TIE2-binding portion (53).

Along with recent studies demonstrating a critical role of TIE2 in diverse human disease models including Ebola hemorrhagic fever (54), anthrax toxicity (55), ocular diseases (56), and vascular leakage model (57), our present study adds evidence for the protective role of TIE2 against diverse pathological conditions characterized by vascular leakage and disintegration. In agreement with our findings, vascular stabilization through activation of Robo4-dependent Slit signaling is also effective against the cytokine storm, alleviating sepsis (7). Thus, we speculate that a therapeutic agent that can induce TIE2 activation can provide a substantial benefit in a broad spectrum of human vascular diseases. The previously reported TIE2 agonists, COMP-Ang1 and Vasculotide, have shown to be effective in various experimental septic models (15, 17–19, 58). However, these agents have a short half-life, requiring frequent administration. In addition, the TIE2-agonistic activity of Vasculotide is under debate (59). In these regard, ABTAA has several merits over the previously known TIE2 agonists. However, because our study indicated that certain concentrations of ANG2, TIE2, and ANG1 are required for the ABTAA-induced TIE2 activation and maintenance of TIE2, there is a possible limitation in cases with no ANG2 elevation, reduced TIE2, or low ANG1 concentrations (20).

In conclusion, we have demonstrated that simultaneous ANG2 inhibition and TIE2 activation by ABTAA are highly effective for strengthening the endothelial barrier, preserving endothelial glycocalyx and microvascular integrity, blunting vascular leakage, and decreasing inflammation in response to sepsis-induced cytokine storm. The approach described here may yield another tool to fight vascular disruption and a way to strengthen the ability to withstand an assault like sepsis.

MATERIALS AND METHODS

Study design
The primary objective of the present study was to investigate the effect of activation of endothelial receptor TIE2 on the vascular integrity and survival of septic mice. To achieve this, we developed a TIE2-activating antibody named ABTAA and elucidated the molecular characteristics of this antibody with extensive in vitro analyses. We then examined the effect of ABTAA on survival in wild-type and several types of conditional knockout mice under three different septic conditions in both therapeutic and preventive settings. Sample size justification was derived from previous animal studies (16, 19) that were sufficiently powered to suggest the possibility of a vascular protection strategy in sepsis. After inducing a septic condition in the mice, the animals were randomized into separate groups for antibody/drug administration. All parameters of genetically modified mice were compared with those of littermate controls. The investigators carrying out the subsequent analyses including survival, morphometric, functional, and biochemical analyses were blind to the information about treatment groups or genotypes.

Additional Materials and Methods are available in the Supplementary Materials.

SUPPLEMENTARY MATERIALS

www.sciencetranslationalmedicine.org/cgi/content/full/8/335/335ra55/DC1
Materials and Methods
Fig. S1. ABTAA binds to human and mouse ANG2.
Fig. S2. ABTAA activates TIE2 and its downstream effectors in human lung ECs.
Fig. S3. ABTAA stimulates internalization of TIE2.
Fig. S4. ABA and ABTAA have different effects on survival of wild-type and $Ang1^{\Delta/\Delta}$ septic mice in the pretreatment setting.
Fig. S5. Constitutive expression of ANG1 is critical for basal and ABTAA-induced TIE2 activity.
Fig. S6. Circulating ANG2 concentrations are very low in $Ang2^{\Delta/\Delta}$ mice.
Fig. S7. ABTAA has a longer half-life and is more effective than COMP-Ang1 for improving survival from sepsis.
Fig. S8. ABTAA protects against major organ injury and microvascular disintegration.
Fig. S9. Pretreatment with ABA or ABTAA mitigates parenchymal injuries and microvascular disintegration.
Fig. S10. Intravital microscopy was used to measure the pulmonary endothelial glycocalyx.
Fig. S11. ABTAA reduces pulmonary vascular leakage.
Fig. S12. Pretreatment with ABTAA blunts the cytokine storm in sepsis.
Fig. S13. Posttreatment with ABTAA does not attenuate cytokine storm in the primary endotoxemia model.
Fig. S14. Pretreatment with ABTAA blunts ANG2 surge in sepsis.
Table S1. Raw data for graphs.
Movie S1. Posttreatment with ABTAA rejuvenates septic mice.
References (60–70)

REFERENCES AND NOTES

1. D. C. Angus, T. van der Poll, Severe sepsis and septic shock. *N. Engl. J. Med.* **369**, 840–851 (2013).
2. N. K. J. Adhikari, R. A. Fowler, S. Bhagwanjee, G. D. Rubenfeld, Critical care and the global burden of critical illness in adults. *Lancet* **376**, 1339–1346 (2010).
3. M. P. Fink, H. S. Warren, Strategies to improve drug development for sepsis. *Nat. Rev. Drug Discov.* **13**, 741–758 (2014).
4. T. van der Poll, S. M. Opal, Host–pathogen interactions in sepsis. *Lancet Infect. Dis.* **8**, 32–43 (2008).
5. V. M. Ranieri, B. T. Thompson, P. S. Barie, J.-F. Dhainaut, I. S. Douglas, S. Finfer, B. Gårdlund, J. C. Marshall, A. Rhodes, A. Artigas, D. Payen, J. Tenhunen, H. R. Al-Khalidi, V. Thompson, J. Janes, W. L. Macias, B. Vangerow, M. D. Williams; PROWESS-SHOCK Study Group, Drotrecogin alfa (activated) in adults with septic shock. *N. Engl. J. Med.* **366**, 2055–2064 (2012).

6. N. M. Goldenberg, B. E. Steinberg, A. S. Slutsky, W. L. Lee, Broken barriers: A new take on sepsis pathogenesis. *Sci. Transl. Med.* **3**, 88ps25 (2011).

7. N. R. London, W. Zhu, F. A. Bozza, M. C. P. Smith, D. M. Greif, L. K. Sorensen, L. Chen, Y. Kaminoh, A. C. Chan, S. F. Passi, C. W. Day, D. L. Barnard, G. A. Zimmerman, M. A. Krasnow, D. Y. Li, Targeting Robo4-dependent Slit signaling to survive the cytokine storm in sepsis and influenza. *Sci. Transl. Med.* **2**, 23ra19 (2010).

8. S. M. Opal, T. van der Poll, Endothelial barrier dysfunction in septic shock. *J. Intern. Med.* **277**, 277–293 (2014).

9. W. L. Lee, A. S. Slutsky, Sepsis and endothelial permeability. *N. Engl. J. Med.* **363**, 689–691 (2010).

10. S. R. Coughlin, Thrombin signalling and protease-activated receptors. *Nature* **407**, 258–264 (2000).

11. W. C. Aird, The role of the endothelium in severe sepsis and multiple organ dysfunction syndrome. *Blood* **101**, 3765–3777 (2003).

12. E. Lemichez, M. Lecuit, X. Nassif, S. Bourdoulous, Breaking the wall: Targeting of the endothelium by pathogenic bacteria. *Nat. Rev. Microbiol.* **8**, 93–104 (2010).

13. N. P. J. Brindle, P. Saharinen, K. Alitalo, Signaling and functions of angiopoietin-1 in vascular protection. *Circ. Res.* **98**, 1014–1023 (2006).

14. H. G. Augustin, G. Y. Koh, G. Thurston, K. Alitalo, Control of vascular morphogenesis and homeostasis through the angiopoietin–Tie system. *Nat. Rev. Mol. Cell Biol.* **10**, 165–177 (2009).

15. S. David, C. C. Ghosh, P. Kümpers, N. Shushakova, P. Van Slyke, E. V. Khankin, S. A. Karumanchi, D. Dumont, S. M. Parikh, Effects of a synthetic PEG-ylated Tie-2 agonist peptide on endotoxemic lung injury and mortality. *Am. J. Physiol. Lung Cell. Mol. Physiol.* **300**, L851–L862 (2011).

16. T. Ziegler, J. Horstkotte, C. Schwab, V. Pfetsch, K. Weinmann, S. Dietzel, I. Rohwedder, R. Hinkel, L. Gross, S. Lee, J. Hu, O. Soehnlein, W. M. Franz, M. Sperandio, U. Pohl, M. Thomas, C. Weber, H. G. Augustin, R. Fässler, U. Deutsch, C. Kupatt, Angiopoietin 2 mediates microvascular and hemodynamic alterations in sepsis. *J. Clin. Invest.* **123**, 3436–3445 (2013).

17. B. Witzenbichler, D. Westermann, S. Knueppel, H.-P. Schultheiss, C. Tschope, Protective role of angiopoietin-1 in endotoxic shock. *Circulation* **111**, 97–105 (2005).

18. S. David, J-K. Park, M. van Meurs, J. G. Zijlstra, C. Koenecke, C. Schrimpf, N. Shushakova, F. Gueler, H. Haller, P. Kümpers, Acute administration of recombinant Angiopoietin-1 ameliorates multiple-organ dysfunction syndrome and improves survival in murine sepsis. *Cytokine* **55**, 251–259 (2011).

19. P. Kümpers, F. Gueler, S. David, P. Van Slyke, D. J. Dumont, J-K. Park, C. L. Bockmeyer, S. M. Parikh, H. Pavenstädt, H. Haller, N. Shushakova, The synthetic Tie2 agonist peptide vasculotide protects against vascular leakage and reduces mortality in murine abdominal sepsis. *Crit. Care* **15**, R261 (2011).

20. S. M. Parikh, Dysregulation of the angiopoietin–Tie-2 axis in sepsis and ARDS. *Virulence* **4**, 517–524 (2013).

21. C-H. Cho, R. A. Kammerer, H. J. Lee, M. O. Steinmetz, Y. S. Ryu, S. H. Lee, K. Yasunaga, K-T. Kim, I. Kim, H.-H. Choi, W. Kim, S. H. Kim, S. K. Park, G. M. Lee, G. Y. Koh, COMP-Ang1: A designed angiopoietin-1 variant with nonleaky angiogenic activity. *Proc. Natl. Acad. Sci. U.S.A.* **101**, 5547–5552 (2004).

22. J. Lee, K. E. Kim, D.-K. Choi, J. Y. Jang, J.-J. Jung, H. Kiyonari, G. Shioi, W. Chang, T. Suda, N. Mochizuki, Y. Nakaoka, I. Komuro, O.-J. Yoo, G. Y. Koh, Angiopoietin-1 guides directional angiogenesis through integrin $\alpha_v\beta_5$ signaling for recovery of ischemic retinopathy. *Sci. Transl. Med.* **5**, 203ra127 (2013).

23. C-H. Cho, K. E. Kim, J. Byun, H.-S. Jang, D.-K. Kim, P. Baluk, F. Baffert, G. M. Lee, N. Mochizuki, J. Kim, B. H. Jeon, D. M. McDonald, G. Y. Koh, Long-term and sustained COMP-Ang1 induces long-lasting vascular enlargement and enhanced blood flow. *Circ. Res.* **97**, 86–94 (2005).

24. U. Fiedler, H. G. Augustin, Angiopoietins: A link between angiogenesis and inflammation. *Trends Immunol.* **27**, 552–558 (2006).

25. U. Fiedler, Y. Reiss, M. Scharpfenecker, V. Grunow, S. Koidl, G. Thurston, N. W. Gale, M. Witzenrath, S. Rosseau, N. Suttorp, A. Sobke, M. Herrmann, K. T. Preissner, P. Vajkoczy, H. G. Augustin, Angiopoietin-2 sensitizes endothelial cells to TNF-α and has a crucial role in the induction of inflammation. *Nat. Med.* **12**, 235–239 (2006).

26. S. David, A. Mukherjee, C. C. Ghosh, M. Yano, E. V. Khankin, J. B. Wenger, S. A. Karumanchi, N. I. Shapiro, S. M. Parikh, Angiopoietin-2 may contribute to multiple organ dysfunction and death in sepsis. *Crit. Care Med.* **40**, 3034–3041 (2012).

27. S. M. Parikh, T. Mammoto, A. Schultz, H.-T. Yuan, D. Christiani, S. A. Karumanchi, V. P. Sukhatme, Excess circulating angiopoietin-2 may contribute to pulmonary vascular leak in sepsis in humans. *PLOS Med.* **3**, e46 (2006).

28. J. M. Siner, V. Bhandari, K. M. Engle, J. A. Elias, M. D. Siegel, Elevated serum angiopoietin 2 levels are associated with increased mortality in sepsis. *Shock* **31**, 348–353 (2009).

29. T. Stiehl, K. Thamm, J. Kaufmann, U. Schaeper, T. Kirsch, H. Haller, A. Santel, C. C. Ghosh, S. M. Parikh, S. David, Lung-targeted RNA interference against angiopoietin-2 ameliorates multiple organ dysfunction and death in sepsis. *Crit. Care Med.* **42**, e654–e662 (2014).

30. J. Lomas-Neira, F. Venet, C-S. Chung, R. Thakkar, D. Heffernan, A. Ayala, Neutrophil–endothelial interactions mediate angiopoietin-2–associated pulmonary endothelial cell dysfunction in indirect acute lung injury in mice. *Am. J. Respir. Cell Mol. Biol.* **50**, 193–200 (2014).

31. J. L. Brown, Z. A. Cao, M. Pinzon-Ortiz, J. Kendrew, C. Reimer, S. Wen, J. Q. Zhou, M. Tabrizi, S. Emery, B. McDermott, L. Pablo, P. McCoon, V. Bedian, D. C. Blakey, A human monoclonal anti-ANG2 antibody leads to broad antitumor activity in combination with VEGF inhibitors and chemotherapy agents in preclinical models. *Mol. Cancer Ther.* **9**, 145–156 (2010).

32. C. C. Leow, K. Coffman, I. Inigo, S. Breen, M. Czapiga, S. Soukharev, N. Gingles, N. Peterson, C. Fazenbaker, R. Woods, B. Jallal, S.-A. Ricketts, T. Lavallee, S. Coats, Y. Chang, MEDI3617, a human anti-angiopoietin 2 monoclonal antibody, inhibits angiogenesis and tumor growth in human tumor xenograft models. *Int. J. Oncol.* **40**, 1321–1330 (2012).

33. J. Oliner, H. Min, J. Leal, D. Yu, S. Rao, E. You, X. Tang, H. Kim, S. Meyer, S. J. Han, N. Hawkins, R. Rosenfeld, E. Davy, K. Graham, F. Jacobsen, S. Stevenson, J. Ho, Q. Chen, T. Hartmann, M. Michaels, M. Kelley, L. Li, K. Sitney, F. Martin, J-R. Sun, N. Zhang, J. Lu, J. Estrada, R. Kumar, A. Coxon, S. Kaufman, J. Pretorius, S. Scully, R. Cattley, M. Payton, S. Coats, L. Nguyen, B. Desilva, A. Ndifor, I. Hayward, R. Radinsky, T. Boone, R. Kendall, Suppression of angiogenesis and tumor growth by selective inhibition of angiopoietin-2. *Cancer Cell* **6**, 507–516 (2004).

34. C. Daly, C. Eichten, C. Castanaro, E. Pasnikowski, A. Adler, A. S. Lalani, N. Papadopoulos, A. H. Kyle, A. I. Minchinton, G. D. Yancopoulos, G. Thurston, Angiopoietin-2 functions as a Tie2 agonist in tumor models, where it limits the effects of VEGF inhibition. *Cancer Res.* **73**, 108–118 (2013).

35. T. Holopainen, P. Saharinen, G. D'Amico, A. Lampinen, L. Eklund, R. Sormunen, A. Anisimov, G. Zarkada, M. Lohela, H. Heloterä, T. Tammela, L. E. Benjamin, S. Ylä-Herttuala, C. C. Leow, G. Y. Koh, K. Alitalo, Effects of angiopoietin-2-blocking antibody on endothelial cell–cell junctions and lung metastasis. *J. Natl. Cancer Inst.* **104**, 461–475 (2012).

36. X. Zhang, L. Gan, H. Pan, S. Guo, X. He, S. T. Olson, A. Mesecar, S. Adam, T. G. Unterman, Phosphorylation of serine 256 suppresses transactivation by FKHR (FOXO1) by multiple mechanisms. Direct and indirect effects on nuclear/cytoplasmic shuttling and DNA binding. *J. Biol. Chem.* **277**, 45276–45284 (2002).

37. K-T. Kim, H-H. Choi, M. O. Steinmetz, B. Maco, R. A. Kammerer, S. Y. Ahn, H.-Z. Kim, G. M. Lee, G. Y. Koh, Oligomerization and multimerization are critical for angiopoietin-1 to bind and phosphorylate Tie2. *J. Biol. Chem.* **280**, 20126–20131 (2005).

38. G. Y. Koh, Orchestral actions of angiopoietin-1 in vascular regeneration. *Trends Mol. Med.* **19**, 31–39 (2013).

39. E. Bogdanovic, V. P. K. H. Nguyen, D. J. Dumont, Activation of Tie2 by angiopoietin-1 and angiopoietin-2 results in their release and receptor internalization. *J. Cell Sci.* **119**, 3551–3560 (2006).

40. D. Rittirsch, M. S. Huber-Lang, M. A. Flierl, P. A. Ward, Immunodesign of experimental sepsis by cecal ligation and puncture. *Nat. Protoc.* **4**, 31–36 (2008).

41. S. D. McCarter, S. H. J. Mei, P. F. H. Lai, Q. W. Zhang, C. H. Parker, R. S. Suen, R. D. Hood, Y. D. Zhao, Y. Deng, R. N. Han, D. J. Dumont, D. J. Stewart, Cell-based angiopoietin-1 gene therapy for acute lung injury. *Am. J. Respir. Crit. Care Med.* **175**, 1014–1026 (2007).

42. S. Weinbaum, J. M. Tarbell, E. R. Damiano, The structure and function of the endothelial glycocalyx layer. *Annu. Rev. Biomed. Eng.* **9**, 121–167 (2007).

43. E. P. Schmidt, Y. Yang, W. J. Janssen, A. Gandjeva, M. J. Perez, L. Barthel, R. L. Zemans, J. C. Bowman, D. E. Koyanagi, Z. X. Yunt, L. P. Smith, S. S. Cheng, K. H. Overdier, K. R. Thompson, M. W. Geraci, I. S. Douglas, D. B. Pearse, R. M. Tuder, The pulmonary endothelial glycocalyx regulates neutrophil adhesion and lung injury during experimental sepsis. *Nat. Med.* **18**, 1217–1223 (2012).

44. A. H. J. Salmon, C. R. Neal, L. M. Sage, C. A. Glass, S. J. Harper, D. O. Bates, Angiopoietin-1 alters microvascular permeability coefficients in vivo via modification of endothelial glycocalyx. *Cardiovasc. Res.* **83**, 24–33 (2009).

45. J. R. Tisoncik, M. J. Korth, C. P. Simmons, J. Farrar, T. R. Martin, M. G. Katze, Into the eye of the cytokine storm. *Microbiol. Mol. Biol. Rev.* **76**, 16–32 (2012).

46. P. Kümpers, M. van Meurs, S. David, G. Molema, J. Bijzet, A. Lukasz, F. Biertz, H. Haller, J. G. Zijlstra, Time course of angiopoietin-2 release during experimental human endotoxemia and sepsis. *Crit. Care* **13**, R64 (2009).

47. J. S. Davis, T. W. Yeo, K. A. Piera, T. Woodberry, D. S. Celermajer, D. P. Stephens, N. M. Anstey, Angiopoietin-2 is increased in sepsis and inversely associated with nitric oxide-dependent microvascular reactivity. *Crit. Care* **14**, R89 (2010).

48. K. A. Shirey, W. Lai, A. J. Scott, M. Lipsky, P. Mistry, L. M. Pletneva, C. L. Karp, J. McAlees, T. L. Gioannini, J. Weiss, W. H. Chen, R. K. Ernst, D. P. Rossignol, F. Gusovsky, G. Blanco, S. N. Vogel, The TLR4 antagonist Eritoran protects mice from lethal influenza infection. *Nature* **497**, 498–502 (2013).

49. H. Wang, H. Liao, M. Ochani, M. Justiniani, X. Lin, L. Yang, Y. Al-Abed, H. Wang, C. Metz, E. J. Miller, K. J. Tracey, L. Ulloa, Cholinergic agonists inhibit HMGB1 release and improve survival in experimental sepsis. *Nat. Med.* **10**, 1216–1221 (2004).

50. K. J. Tracey, Y. Fong, D. G. Hesse, K. R. Manogue, A. T. Lee, G. C. Kuo, S. F. Lowry, A. Cerami, Anti-cachectin/TNF monoclonal antibodies prevent septic shock during lethal bacteraemia. *Nature* **330**, 662–664 (1987).

51. E. J. Kerschen, J. A. Fernandez, B. C. Cooley, X. V. Yang, R. Sood, L. O. Mosnier, F. J. Castellino, N. Mackman, J. H. Griffin, H. Weiler, Endotoxemia and sepsis mortality reduction by non-anticoagulant–activated protein C. *J. Exp. Med.* **204**, 2439–2448 (2007).

52. J. H. Kang, M. Super, C. W. Yung, R. M. Cooper, K. Domansky, A. R. Graveline, T. Mammoto, J. B. Berthet, H. Tobin, M. J. Cartwright, A. L. Watters, M. Rottman, A. Waterhouse, A. Mammoto, N. Gamini, M. J. Rodas, A. Kole, A. Jiang, T. M. Valentin, A. Diaz, K. Takahashi, D. E. Ingber, An extracorporeal blood-cleansing device for sepsis therapy. *Nat. Med.* **20**, 1211–1216 (2014).

53. W. A. Barton, D. Tzvetkova-Robev, E. P. Miranda, M. V. Kolev, K. R. Rajashankar, J. P. Himanen, D. B. Nikolov, Crystal structures of the Tie2 receptor ectodomain and the angiopoietin-2–Tie2 complex. *Nat. Struct. Mol. Biol.* **13**, 524–532 (2006).

54. A. L. Rasmussen, A. Okumura, M. T. Ferris, R. Green, F. Feldmann, S. M. Kelly, D. P. Scott, D. Safronetz, E. Haddock, R. LaCasse, M. J. Thomas, P. Sova, V. S. Carter, J. M. Weiss, D. R. Miller, G. D. Shaw, M. J. Korth, M. T. Heise, R. S. Baric, F. P.-M. de Villena, H. Feldmann, M. G. Katze, Host genetic diversity enables Ebola hemorrhagic fever pathogenesis and resistance. *Science* **346**, 987–991 (2014).

55. C. C. Ghosh, A. Mukherjee, S. David, U. G. Knaus, D. J. Stearns-Kurosawa, S. Kurosawa, S. M. Parikh, Impaired function of the Tie-2 receptor contributes to vascular leakage and lethality in anthrax. *Proc. Natl. Acad. Sci. U.S.A.* **109**, 10024–10029 (2012).

56. J. Shen, M. Frye, B. L. Lee, J. L. Reinardy, J. M. McClung, K. Ding, M. Kojima, H. Xia, C. Seidel, R. Lima e Silva, A. Dong, S. F. Hackett, J. Wang, B. W. Howard, D. Vestweber, C. D. Kontos, K. G. Peters, P. A. Campochiaro, Targeting VE-PTP activates TIE2 and stabilizes the ocular vasculature. *J. Clin. Invest.* **124**, 4564–4576 (2014).

57. G. T. Thurston, J. S. Rudge, E. Ioffe, H. Zhou, L. Ross, S. D. Croll, N. Glazer, J. Holash, D. M. McDonald, G. D. Yancopoulos, Angiopoietin-1 protects the adult vasculature against plasma leakage. *Nat. Med.* **6**, 460–463 (2000).

58. M. G. Sugiyama, S. M. Armstrong, C. Wang, D. Hwang, H. Leong-Poi, A. Advani, S. Advani, H. Zhang, K. Szaszi, A. Tabuchi, W. M. Kuebler, P. Van Slyke, D. J. Dumont, W. L. Lee, The Tie2-agonist Vasculotide rescues mice from influenza virus infection. *Sci. Rep.* **5**, 11030 (2015).

59. F. T. H. Wu, C. R. Lee, E. Bogdanovic, A. Prodeus, J. Gariépy, R. S. Kerbel, Vasculotide reduces endothelial permeability and tumor cell extravasation in the absence of binding to or agonistic activation of Tie2. *EMBO Mol. Med.* **7**, 770–787 (2015).

60. H. Y. Yang, K. J. Kang, J. E. Chung, H. Shim, Construction of a large synthetic human scFv library with six diversified CDRs and high functional diversity. *Mol. Cells* **27**, 225–235 (2009).

61. G. Thurston, C. Daly, U.S. Patent 12/843,905 (2010).

62. S.-J. Hwang, S. H. Kim, H.-Z. Kim, M. O. Steinmetz, G. Y. Koh, G. M. Lee, High-level expression and purification of a designed angiopoietin-1 chimeric protein, COMP-Ang1, produced in Chinese hamster ovary cells. *Protein J.* **27**, 319–326 (2008).

63. Y. Arita, Y. Nakaoka, T. Matsunaga, H. Kidoya, K. Yamamizu, Y. Arima, T. Kataoka-Hashimoto, K. Ikeoka, T. Yasui, T. Masaki, K. Yamamoto, K. Higuchi, J.-S. Park, M. Shirai, K. Nishiyama, H. Yamagishi, K. Otsu, H. Kurihara, T. Minami, K. Yamauchi-Takihara, G. Y. Koh, N. Mochizuki, N. Takakura, Y. Sakata, J. K. Yamashita, I. Komuro, Myocardium-derived angiopoietin-1 is essential for coronary vein formation in the developing heart. *Nat. Commun.* **5**, 4552 (2014).

64. B. Shen, Z. Shang, B. Wang, L. Zhang, F. Zhou, T. Li, M. Chu, H. Jiang, Y. Wang, T. Qiao, J. Zhang, W. Sun, X. Kong, Y. He, Genetic dissection of tie pathway in mouse lymphatic maturation and valve development. *Arterioscler. Thromb. Vasc. Biol.* **34**, 1221–1230 (2014).

65. S. Savant, S. La Porta, A. Budnik, K. Busch, J. Hu, N. Tisch, C. Korn, A. F. Valls, A. V. Benest, D. Terhardt, X. Qu, R. H. Adams, H. S. Baldwin, C. Ruiz de Almodóvar, H.-R. Rodewald,

66. H. G. Augustin, The orphan receptor Tie1 controls angiogenesis and vascular remodeling by differentially regulating Tie2 in tip and stalk cells. *Cell Rep.* **12**, 1761–1773 (2015).

67. M. R. Looney, E. E. Thornton, D. Sen, W. J. Lamm, R. W. Glenny, M. F. Krummel, Stabilized imaging of immune surveillance in the mouse lung. *Nat. Methods* **8**, 91–96 (2011).

68. K. Choe, J. Y. Jang, I. Park, Y. Kim, S. Ahn, D.-Y. Park, Y.-K. Hong, K. Alitalo, G. Y. Koh, P. Kim, Intravital imaging of intestinal lacteals unveils lipid drainage through contractility. *J. Clin. Invest.* **125**, 4042–4052 (2015).

69. A. Constantinescu, J. A. E. Spaan, E. K. Arkenbout, H. Vink, J. W. G. E. vanTeeffelen, Degradation of the endothelial glycocalyx is associated with chylomicron leakage in mouse cremaster muscle microcirculation. *Thromb. Haemost.* **105**, 790–801 (2011).

70. T. Itoh, H. Obata, S. Murakami, K. Hamada, K. Kangawa, H. Kimura, N. Nagaya, Adrenomedullin ameliorates lipopolysaccharide-induced acute lung injury in rats. *Am. J. Physiol. Lung Cell. Mol. Physiol.* **293**, L446–L452 (2007).

71. M. J. Sung, D. H. Kim, Y. J. Jung, K. P. Kang, A. S. Lee, S. Lee, W. Kim, M. Davaatseren, J.-T. Hwang, H.-J. Kim, M. S. Kim, D. Y. Kwon, S. K. Park, Genistein protects the kidney from cisplatin-induced injury. *Kidney Int.* **74**, 1538–1547 (2008).

Citation: S. Han, S.-J. Lee, K. E. Kim, H. S. Lee, N. Oh, I. Park, E. Ko, S. J. Oh, Y.-S. Lee, D. Kim, S. Lee, D. H. Lee, K.-H. Lee, S. Y. Chae, J.-H. Lee, S.-J. Kim, H.-C. Kim, S. Kim, S. H. Kim, C. Kim, Y. Nakaoka, Y. He, H. G. Augustin, J. Hu, P. H. Song, Y.-I. Kim, P. Kim, I. Kim, G. Y. Koh, Amelioration of sepsis by TIE2 activation–induced vascular protection. *Sci. Transl. Med.* **8**, 335ra55 (2016).

Editor's Summary

Antibody TIEs sepsis up in knots

Sepsis, or severe systemic inflammation caused by infection, has a high mortality despite the availability of antibiotic treatment, and more specific therapies are urgently needed. One of the difficult-to-treat and potentially life-threatening components of sepsis is vascular disintegration and leakage. Han *et al*. have discovered an antibody, called ABTAA, which binds to a ligand called angiopoietin 2 (ANG2) in the vasculature, but then activates it instead of blocking its activity like standard antibodies. When ABTAA binds to ANG2, it causes clustering of ANG2 and subsequently its receptor TIE2 at the site, and the resulting signaling cascade protects the vascular walls and blunts the damaging effects of sepsis, greatly increasing survival in mouse models of the disease.

The following resources related to this article are available online at http://stm.sciencemag.org.
This information is current as of April 20, 2016.

Article Tools	Visit the online version of this article to access the personalization and article tools: http://stm.sciencemag.org/content/8/335/335ra55
Supplemental Materials	*"Supplementary Materials"* http://stm.sciencemag.org/content/suppl/2016/04/18/8.335.335ra55.DC1
Related Content	The editors suggest related resources on *Science*'s sites: http://stm.sciencemag.org/content/scitransmed/8/335/335fs9.full http://stm.sciencemag.org/content/scitransmed/8/327/327ra25.full http://stm.sciencemag.org/content/scitransmed/7/303/303ra140.full http://stm.sciencemag.org/content/scitransmed/7/299/299ra122.full http://stm.sciencemag.org/content/scitransmed/7/287/287ra71.full
Permissions	Obtain information about reproducing this article: http://www.sciencemag.org/about/permissions.dtl